

radiative heating to drive mean vertical motion sufficient to produce runoff from the Sahara equivalent to 1 m of precipitation per year. Hint: Equate the vertical transport of water vapor at the top of the boundary layer with the precipitation rate  $P$ , e.g.,  $(w\rho_a q)_{1\text{ km}} = P\rho_w$ , where  $\rho_a$  and  $\rho_w$  are the density of air and liquid water, respectively, and  $q$  is the mass mixing ratio of water vapor. Compare your result with the net radiation over the Amazon Basin during the rainy season (Fig. 2.11).

## Chapter 7

# The Ocean General Circulation and Climate

### 7.1 Cauldron of Climate

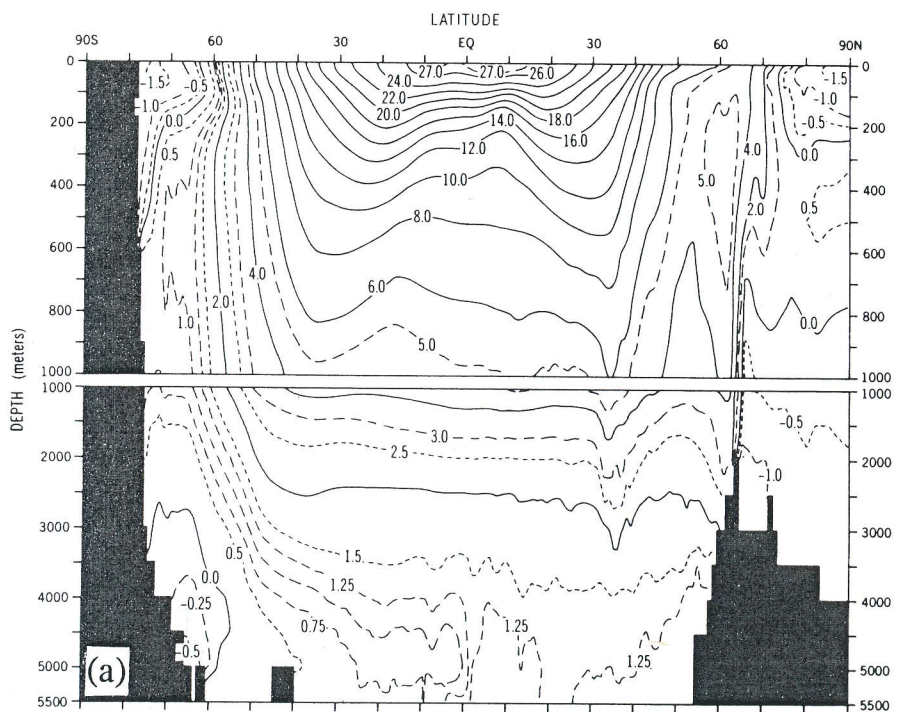
The global ocean plays several critical roles in the physical climate system of Earth. These roles are related to key physical properties of the ocean: it is wet, it has a low albedo, it has a large heat capacity, and it is a fluid. Oceans provide a perfectly wet surface, which when unfrozen has a low albedo and is therefore an excellent absorber of solar radiation. The oceans receive more than half of the energy entering the climate system, and evaporative cooling balances much of the solar energy absorbed by the oceans, making them the primary source of water vapor and heat for the atmosphere. The world ocean is thus the boiler that drives the global hydrologic cycle. The world ocean also provides the bulk of the thermal inertia of the climate system on time scales from weeks to centuries. The great capacity of the oceans to store heat reduces the magnitude of the seasonal cycle in surface temperature by storing heat in summer and releasing it in winter. Because seawater is a fluid, currents in the ocean can move water over great distances and carry heat and other ocean properties from one geographic area to another. The equator-to-pole energy transport by the ocean is important in reducing the pole-to-equator temperature gradient. Horizontal and vertical transport of energy by the ocean can also alter the nature of regional climates by controlling the local sea surface temperature.

In addition to its direct physical effects on the climate system, the global ocean can affect the climate indirectly through chemical and biological processes. The ocean is a large reservoir for the chemical elements that form the atmosphere. Exchange of gases across the air-sea interface controls the concentration of trace chemical species containing oxygen, carbon, sulfur, and nitrogen, which are important in determining the radiative and chemical characteristics of the atmosphere. For example, the ocean controls the concentration of carbon dioxide in the atmosphere by exchanging gaseous carbon dioxide across the air-sea interface. Carbon dioxide is converted to organic solids in the ocean, and carbon is then stored by deposition of these solids onto the sea floor. Sulfur-bearing gases released from biological and chemical processes in the ocean enter the atmosphere where they are converted to aerosols that form the nuclei on which cloud droplets form. Evaporation of sea spray also forms salt particles that can form cloud condensation nuclei. The cloud condensation nuclei produced in the ocean can have a substantial influence on the energy balance of Earth, through their effect on the optical properties and extent of clouds.

## 7.2 Properties of Seawater

Oceanic currents and the resulting heat transports are determined primarily by the physical properties of the ocean. To specify the physical state of seawater requires three variables: pressure, temperature, and salinity. As described in Chapter 1, *salinity* is the mass of dissolved salts in a kilogram of seawater, and is generally measured in parts per thousand, which we denote with the symbol ‰. The average salinity and temperature of the world ocean are approximately 34.7‰ and 3.6°C, respectively. The effect of the ocean on atmospheric composition through biological and chemical processes depends on a more complex mix of physical, chemical, and biological properties. For example, the oxygen and nutrient content of seawater are of critical importance for life in the sea. Trace amounts of key minerals may be very important for local biological productivity.

Only about the first kilometer of ocean between 50°N and 50°S is warmer than 5°C [Fig. 7.1(a)], so that much of the mass of the ocean is between -2°C and 5°C. The thermal structure of the ocean at most locations can be divided into three vertical sections. The top 20–200 m of water in contact with the atmosphere usually has



an almost uniform temperature, which is maintained by rapid mixing through mechanical stirring and thermal overturning. This layer is called the surface *mixed layer* of the ocean. Below the mixed layer the temperature decreases relatively quickly with depth to about 1000 m (Fig. 1.10). This layer of rapid temperature change, called the *permanent thermocline*, persists in all seasons. It is believed that the permanent thermocline is maintained by heating from above, balanced by a slow upward movement of colder water from below. The cold water in the deep abyss of the oceans is produced at the surface in a few regions of the polar ocean. At the base of the permanent thermocline the typical temperature is about 5°C, and below this the temperature decreases more slowly with depth, reaching a temperature of about 2°C in the deepest layers of the ocean. The physical properties of the deep ocean show little spatial variability, so that temperature, salinity, and density are almost uniform (Fig. 7.1).

Water is almost incompressible, so the density of seawater is always very close to  $1000 \text{ kg m}^{-3}$ , even near the bottom of the ocean where the pressure may be several thousand times the surface air pressure. Density of seawater is usually reported as a deviation from  $1000 \text{ kg m}^{-3}$ ,  $\rho_t - 1000$ . *Potential density*,  $\rho_t$ , is the density that seawater with a particular salinity and temperature would have at zero water pressure, or the density at surface air pressure. Potential density increases most rapidly with depth in the first several hundred meters of the tropical and midlatitude ocean [Fig. 7.1(c)]. This rapid increase of density with depth is supported by the absorption of solar radiation near the surface, which sustains the warm temperatures there. The strong density stratification in the upper ocean inhibits vertical motion and turbulent exchanges, so that the deep ocean is somewhat isolated from surface influences in those regions where this density stratification is present. The strong density stratification is reduced in high latitudes, where in some locations (e.g., 65°N and 75°S) the potential density at the surface comes much closer to the densities prevailing in the deep ocean. The distribution of potential density suggests that the water occupying the bulk of the deep ocean came from the polar regions, where at certain locations and seasons surface water becomes dense enough to sink to great depth. The distributions of other tracers also suggest that slow downward motion of water in high latitudes extends downward and equatorward into the deep ocean, as will be discussed in Section 7.6.

Variations of density on pressure surfaces are important for driving the circulation of the ocean, and depend on the temperature and salinity. Salt content increases the density of water, and seawater expands and becomes less dense as its temperature increases. The salinity of seawater ranges from about 25 to 40‰ and the temperature ranges from about -2 to 30°C. By varying within these ranges salinity and temperature have roughly equal importance for density variations in the ocean (Fig. 7.2). The density of seawater is very nearly linearly dependent on salinity. The dependence of density on temperature does not have this simple linear behavior, however. When the temperature of water approaches its freezing point, its density generally

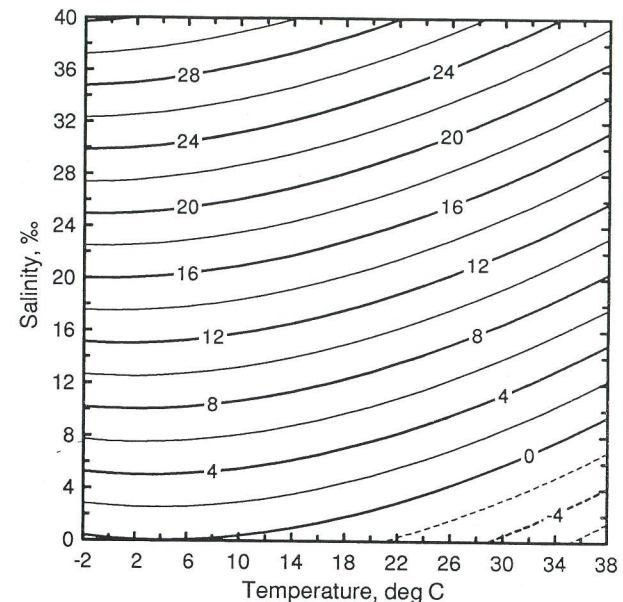


**Fig. 7.2** Contours of seawater density anomalies ( $\rho_t - 1000, \text{kg m}^{-3}$ ) plotted against salinity and temperature.

becomes less sensitive to temperature. For pure water, for example, the maximum density occurs at 4°C, and the water then expands slightly as it is cooled further. Therefore, fresh water lakes that are cooled from the top continue to overturn convectively until the entire water column reaches 4°C, because water that is at 4°C will always be more dense than warmer water. When the entire water column is cooled to 4°C, surface water that is cooled further will become less dense than the column and will "float" at the surface. When it reaches 0°C the surface water will freeze and form a layer of surface ice, which provides a layer of insulation between the cold air above and the warmer water below. If the lake is deep enough, the water near the bottom will remain at about 4°C, although the air temperature above the surface ice may fall to many degrees below zero. This fact allows fish in high-latitude or high-altitude lakes to survive the winter in the liquid water beneath the surface ice.

For seawater with salinity greater than 24.7‰, the density continues to increase with decreasing temperature until freezing occurs, although more slowly as the freezing point is approached. Therefore, if the salinity is initially well mixed, the entire water column must be cooled to the freezing point before ice can form. Sea ice is able to form in the high-latitude oceans because the salinity decreases significantly near the surface (Fig. 1.11). Lower salinities near the surface cause a decrease in

density that offsets the increase in density associated with colder temperatures near the surface, allowing water near the surface to freeze while warmer water is present below. The low surface salinities result primarily from the excess of precipitation over evaporation in these latitudes. In the Arctic Ocean the supply of freshwater from rivers flowing from the surrounding continents contributes importantly to low surface salinities and therefore to the stable density gradient. Because salinity increases with depth, the surface is able to form ice without bringing the temperature of the entire water column to the freezing point. It has been hypothesized that, if the flow of certain key rivers were diverted from the Arctic Ocean to supply irrigation water to continental interiors farther south, the heat balance of the Arctic could be severely distorted, because the normal configuration of a thin layer of surface ice on a mostly unfrozen Arctic Ocean may no longer be stable. Increased salinity of surface waters in the Arctic might lead to either complete removal of most arctic sea ice or complete freezing of the Arctic Ocean from surface to bottom.

### 7.3 The Mixed Layer

The primary heat source for the ocean is solar radiation entering through the top surface. Almost all of the solar energy flux into the ocean is absorbed in the top 100 m. Infrared and near-infrared radiation are absorbed in the top centimeter, but blue and green visible radiation can penetrate to more than 100 m if the water is especially clear. The depth to which visible radiation penetrates the ocean depends on the amount and optical properties of suspended organic matter in the water, which vary greatly with location, depending on the currents and the local biological productivity. The principal component of suspended matter in surface water is *plankton*, which are plants and animals that drift in the near-surface waters of the ocean (Fig. 7.3). The solar flux and heating rate in the ocean are greatest at the surface and decrease exponentially with depth, in accord with the Lambert–Bouguet–Beer Law as described in Chapter 3. Under average conditions the solar flux and heating rate are reduced to half of their surface value by a depth of about one meter, but significant heating can still be present at more than 100 m below the surface.

Since the solar heating is deposited over a depth of several tens of meters in the upper layers of the ocean, and cooling by evaporation and sensible heat transfer to the atmosphere occurs at the surface, there must be an upward flux of energy in the upper ocean to maintain an energy balance between surface loss terms and subsurface heating. Molecular diffusion is an important heat transport mechanism only in the top centimeter of the ocean. Elsewhere the heat flux is carried by turbulent mixing, convective overturning, and mean vertical motion, which is called *upwelling* or *downwelling* in the ocean. Turbulent mixing in the surface layer of the ocean is greatly aided by the supply of mechanical energy by the winds and

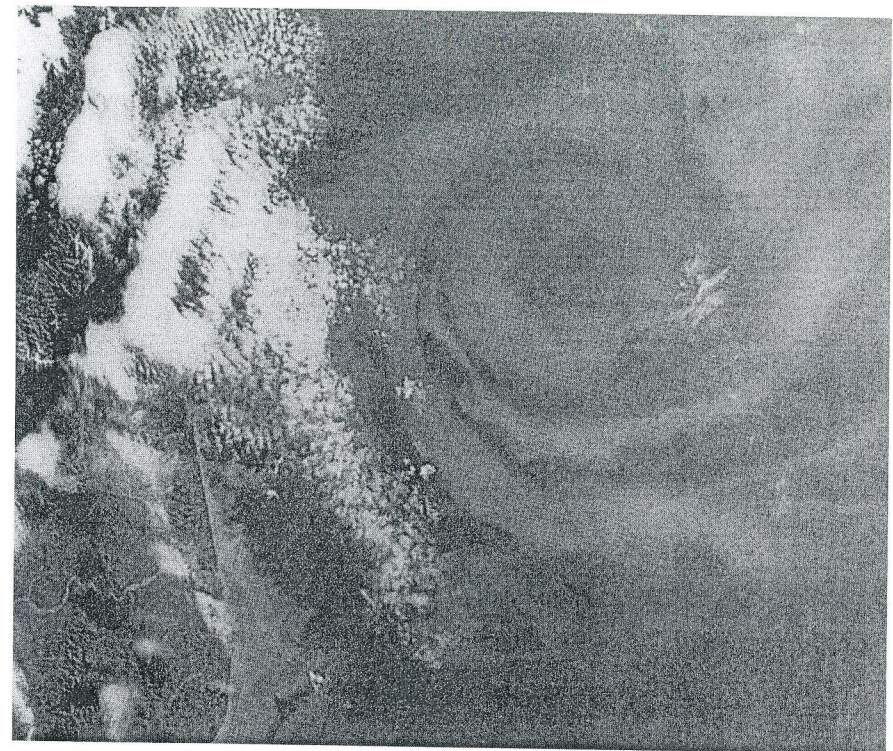


**Fig. 7.3** A small oceanic eddy off New Zealand's South Island, northeast of Christchurch. The variations in water color are associated with the abundance of plankton. The brightest areas are clouds. (Challenger 9, 61A, NASA, October 30, 1985–November 6, 1985.)

their interaction with waves on the surface of the water. In the mixed layer of the ocean, heat transport by convection and turbulent mixing is so efficient that the temperature, salinity, and other properties of the seawater are almost independent of depth (Fig. 7.4).

A schematic diagram showing the processes important in the oceanic mixed layer is presented in Fig. 7.5. The depth of the mixed layer depends on the rate of buoyancy generation and the rate at which kinetic energy is supplied to the ocean surface by winds. If the surface is cooled very strongly, such as at high latitudes during fall and winter, then cold, dense water is formed near the surface at a rapid rate and buoyancy forces will drive convection, with sinking of cold water and rising of warmer water in the mixed layer. When the surface is cooled only weakly or actually heated, such as during summer, when surface solar heating rates are greatest, then the generation of mixing by buoyancy is less and the mixed layer will become thinner and warmer. Buoyancy can be generated by the effect of evaporation on surface

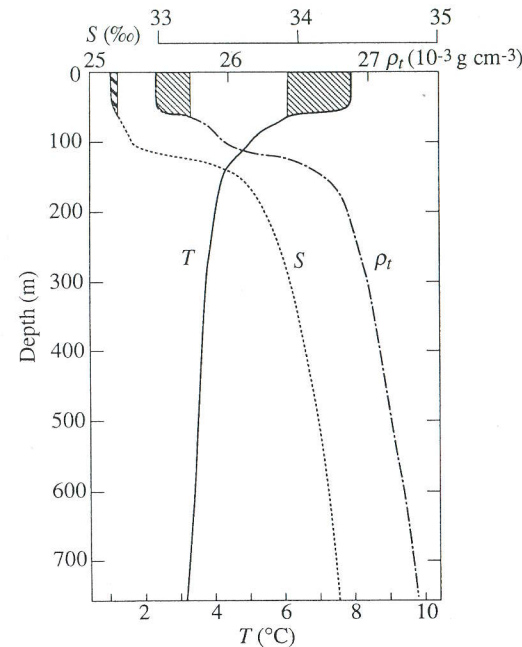


Fig. 7.4 Vertical profiles of temperature ( $T$ ,  $^{\circ}\text{C}$ ), salinity ( $S$ , ‰), and potential density ( $\rho_t - 1000$ ,  $\text{kg m}^{-3}$ ) at Ocean Station P,  $50^{\circ}\text{N}$ ,  $145^{\circ}\text{W}$ , on June 23, 1970 showing the mixed layer in the top 50 m. The hatched area shows the change since May 19, 1970 and indicates the springtime warming and thinning of the mixed layer. [From Denman and Miyake (1973). Reprinted with permission from the American Meteorological Society.]

salinity, even when surface temperatures are increasing with time. The density increase associated with increasingly saline surface waters can balance or overcome thermal stratification and encourage mixing. Rainfall represents an input of freshwater at the surface, which acts to decrease the density of the surface waters. Winds blowing over the ocean waves transfer kinetic energy to the water that results in turbulent water motion as well as mean ocean currents. The supply of turbulent kinetic energy to the upper ocean by winds can induce mixing even in the presence of stable density stratification. If the intensity of turbulence in the mixed layer is great enough, cool, dense water can be entrained into the mixed layer from below. This implies a downward heat transport, which cools and deepens the mixed layer.

The heat, momentum, and moisture exchanges between the atmosphere and the ocean are accomplished through contact of the atmospheric boundary layer with the mixed layer of the ocean. Storage and removal of heat from the ocean on time scales of less than a year are confined to the mixed layer over much of the ocean. The depth of the oceanic mixed layer varies from a few meters in regions where subsurface

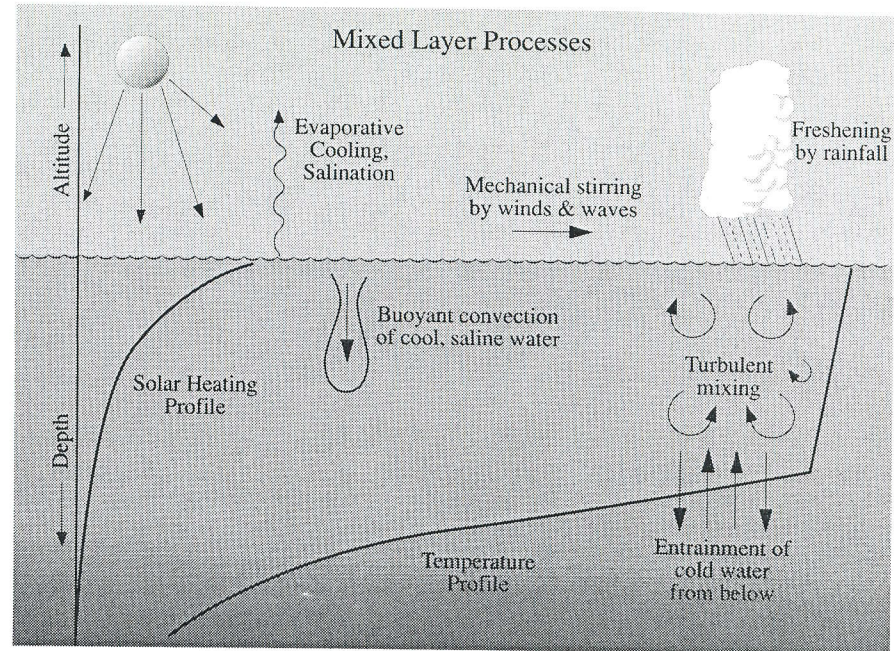
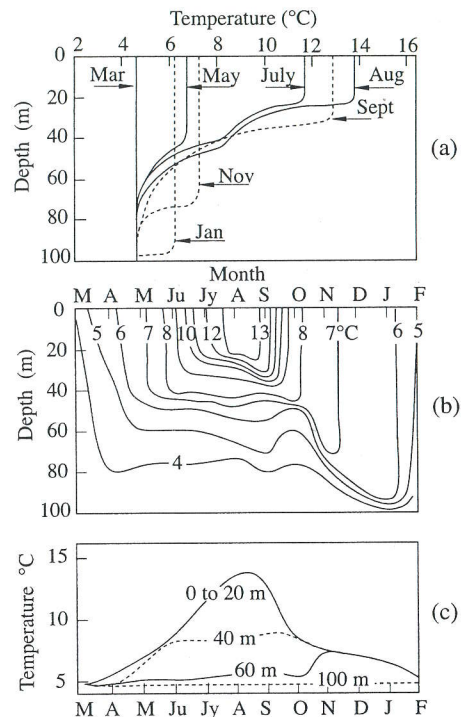


Fig. 7.5 Diagram showing important mixed-layer processes.

water upwells, as along the equator and in eastern boundary currents, to the depth of the ocean in high-latitude regions where cold, saline surface water can sink all the way to the ocean bottom. Regions where the mixed layer is deeper than 500 m constitute a small fraction of the global ocean area, however. In general, as one would expect, the mixed layer is thin where the ocean is being heated and thick where the ocean gives up its energy to the atmosphere. The global-average depth of the mixed layer is about 70 m. The mixed layer responds fairly quickly to changes in surface wind and temperature, whereas the ocean below the mixed layer does not. The thermal capacity of the mixed layer is the effective heat capacity of the ocean on time scales of years to a decade, and is about 30 times the heat capacity of the atmosphere (see Chapter 4).

The oceanic mixed layer responds strongly to the annual cycle of insolation and surface weather. Figure 7.6 shows an example from the midlatitude Pacific Ocean. The mixed layer is warmest and thinnest in late summer near the end of the period of greatest insolation and least intense stirring of the ocean by winds. After August the surface begins to cool, the storminess increases, and the mixed layer begins to deepen and cool. The mixed layer continues to deepen and cool throughout the winter, and by the end of winter may extend to a depth of several hundred meters and merge



**Fig. 7.6** Seasonal variation of temperature in the upper ocean at 50°N, 145°W in the eastern north Pacific. (a) Vertical profiles of temperature by months, (b) temperature contours, and (c) temperatures at various depths versus time of year. [From Pickard and Emery (1990). Reprinted with permission from Pergamon Press, Ltd., Oxford, England.]

smoothly into the permanent thermocline. During most of the rest of the year a seasonal thermocline with steep temperature gradients links the permanent thermocline with the base of the mixed layer. In spring and summer this seasonal thermocline develops and the mixed layer becomes thinner and warmer. Seasonal variations in temperature are confined primarily to the mixed layer and the seasonal thermocline, so those temperatures at depths below the deepest extent of the mixed layer experience little seasonal variation.

#### 7.4 The Wind-Driven Circulation

The transfer of momentum from winds to ocean currents plays a critical role in driving the circulation of the ocean. This is particularly true for the currents near the

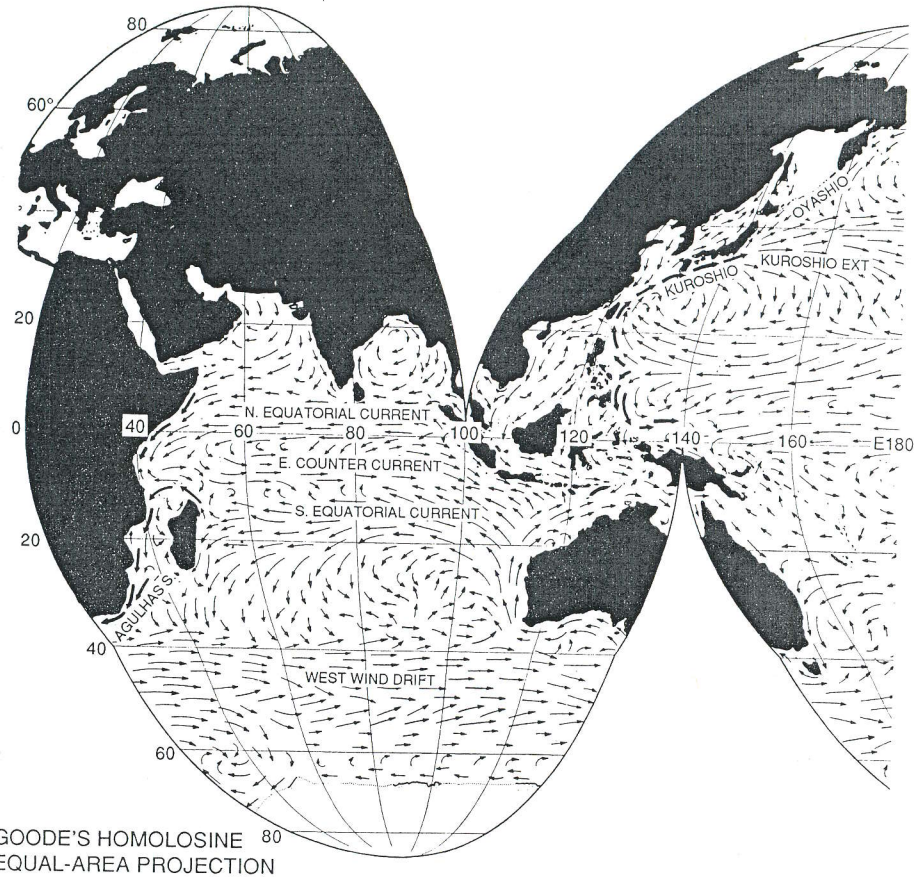


**Fig. 7.7** Map of surface currents. (*Figure continues.*) [Adapted from Sverdrup *et al.* (1942).]

ocean surface. The general character of the large-scale surface ocean currents is shown in Fig. 7.7. The surface currents are arranged in coherent patterns with large circulations called *gyres* occupying the major ocean basins. In addition, many narrow but persistent currents appear in time-averaged maps.

##### 7.4.1 Western Boundary Currents

Some of the most visible current structures are the large clockwise circulations in the northern Pacific and Atlantic oceans. Along the western boundaries of the Pacific and Atlantic Ocean basins strong poleward-flowing currents exist in a narrow zone

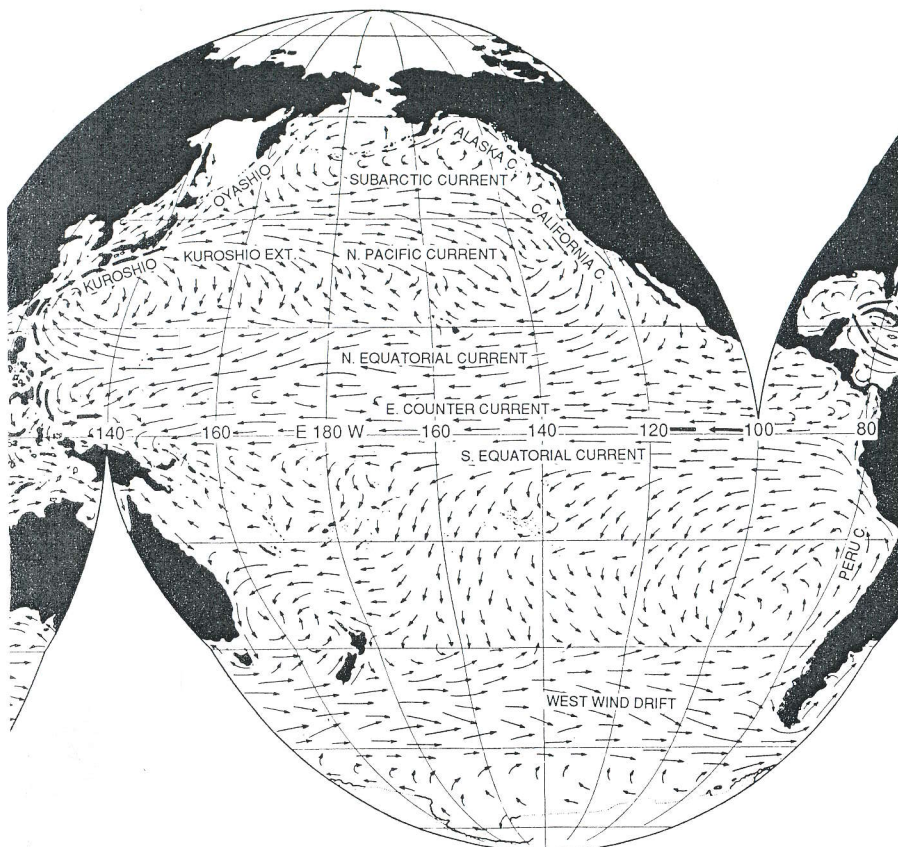


Fig. 7.7—Continued

very near the continents. These currents are called the Kuroshio and the Gulf Stream, respectively, and may be referred to generically as western boundary currents. Western boundary currents also occur in the Southern Hemisphere along South America (Brazil Current) and along Africa (Agulhas Stream). They are generally less sharply defined and extensive in the Southern Hemisphere, perhaps because of the different ocean geometry that allows the Antarctic circumpolar current to flow unimpeded in a continuous eastward current at about 60°S. Western boundary currents carry warm water from the tropics to middle latitudes. The speed of these currents may exceed one meter per second, which is quite fast for an ocean current. With the possible exceptions of the Antarctic circumpolar current and some zonal equatorial currents, these currents are the closest oceanographic analog to the jet streams of the atmosphere, although they flow poleward rather than eastward. The return flow of water

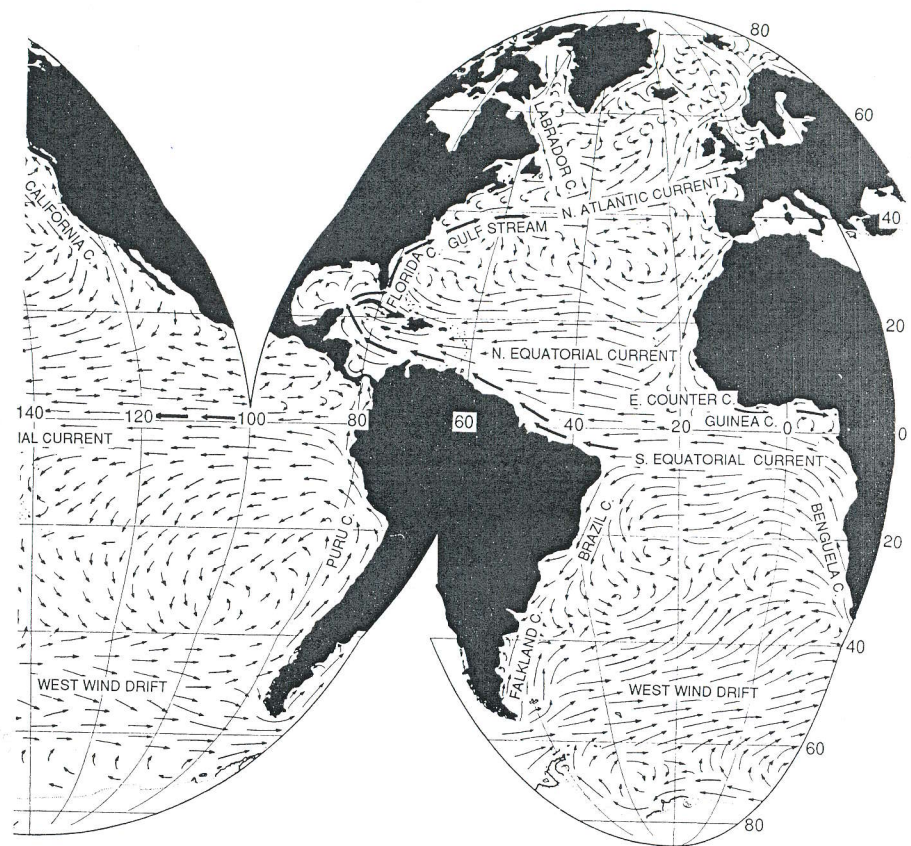
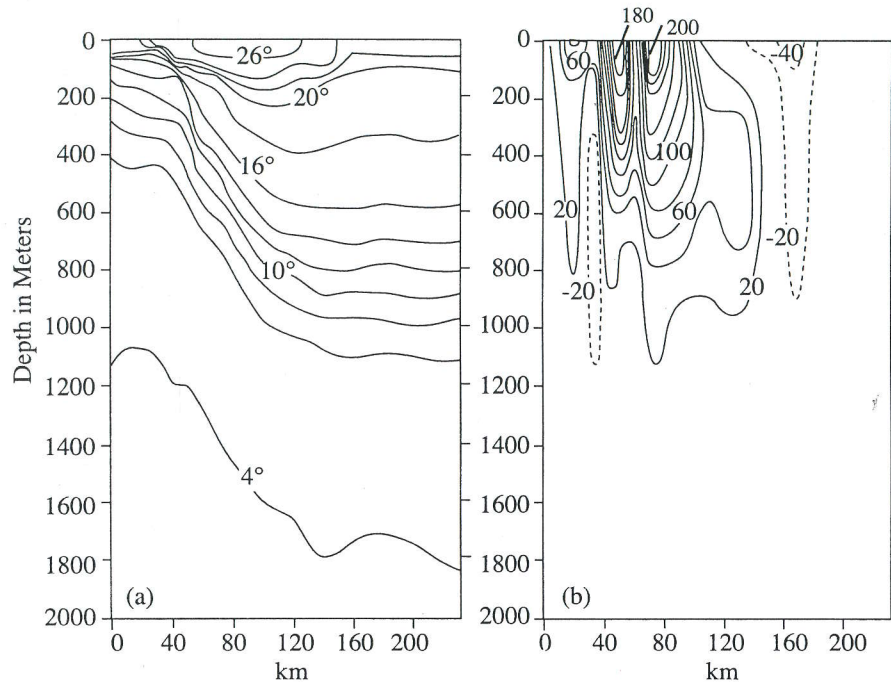


Fig. 7.7—Continued

from midlatitudes to the equator is much more gradual and occurs in a broad expanse across the center of each basin.

The thermal-current structure of the Gulf Stream after it has left the coast at Cape Hatteras and is flowing approximately east is shown in Fig. 7.8. The warmest water occurs near the surface coincident with the strongest current velocities, which are near  $2 \text{ m s}^{-1}$ . These strong currents are accompanied by strong subsurface temperature gradients across the stream, with warmer water to the south and east of the current and cooler water to the north and west. These temperature gradients persist when the current leaves the western margin of the ocean and flows into the interior of the ocean basin. The current is not straight or steady, but breaks down into meanders and rings and eventually loses a clear identity as the flow expands eastward across the basin (Fig. 7.9).



**Fig. 7.8** Cross section of temperature (contour interval  $2^{\circ}\text{C}$ ) and geostrophic current (contour interval  $20 \text{ cm s}^{-1}$ ) across the Gulf Stream at about  $38^{\circ}\text{N}$ ,  $68^{\circ}\text{W}$ . [From Stommel (1965), adapted from Worthington (1954). Reprinted with permission from Munksgaard International Publishers Ltd.]

The poleward flux of warm water in the Gulf Stream and Kuroshio currents has a profound effect on the *sea surface temperature* (SST) and the climate of the land areas bordering the oceans, especially the lands immediately downwind of the oceans. The averaged sea surface temperature distribution for DJF [Fig. 7.10(a)] shows a strong gradient in the north Atlantic Ocean aligned approximately with the mean position of the Gulf Stream. This strong temperature gradient extends northeastward from the mid-Atlantic coast of North America to the Norwegian Sea in the vicinity of Spitzbergen. It appears that some of the heat carried northward by the Gulf Stream is picked up by the Norwegian Current and carried into polar latitudes. As a result, at middle and high latitudes the eastern Atlantic is much warmer at the surface than the western Atlantic Ocean. This asymmetry in the Atlantic sea surface temperature contributes to the milder winter climates of western European land areas compared to eastern North American land areas at the same latitude. Another major contribution to this climate asymmetry is the eastward advection of temperature in the atmosphere.



**Fig. 7.9** Gray-scale image of SST in the northwestern Atlantic showing meanders and rings in the Gulf Stream. Warm water is light in color. (Courtesy of Dr. O. Brown, University of Miami.)

#### 7.4.2 Eastern Boundary Currents

Also important for climate are eastern boundary currents, which occur in tropical and subtropical latitudes at the eastern margins of the oceans. The names given to the eastern boundary currents in these geographic areas are the California Current off North America, the Peru Current off South America, the Lewin Current off eastern Australia, the Canary Current off northern Africa, and the Benguela Current off southern Africa. In each of these regions a wind-driven current flows along the coast toward the equator and then turns westward toward the center of the basin. These currents are associated with cold SST, which can be illustrated by

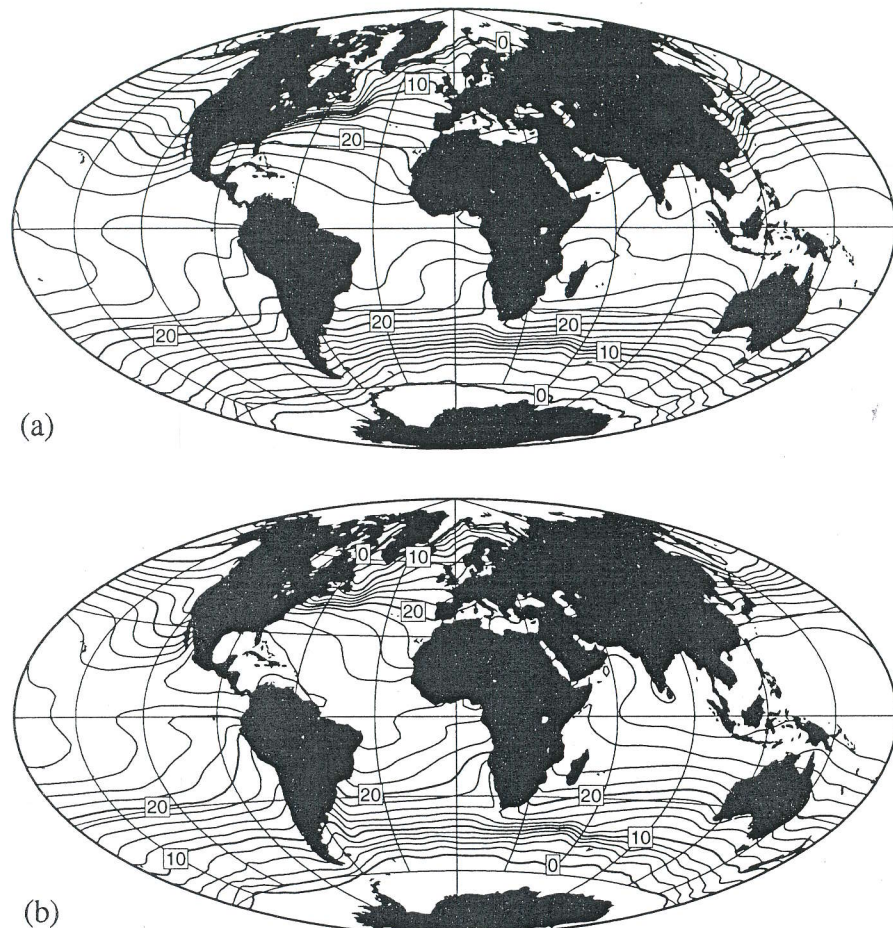


**Fig. 7.10** Average (a) December–February (DJF) and (b) June–August (JJA) sea surface temperature ( $^{\circ}\text{C}$ ).

plotting the deviation of SST from its average at each latitude (Fig. 7.11). The SST in the subtropics to the west of the continents in the Atlantic and Pacific Oceans is much colder than the zonal average at each latitude. The coldest water occurs very near the coast and extends westward and equatorward into the oceans. The low SST near the coast is produced by upwelling of cold subsurface waters, which is driven by alongshore or offshore winds in these regions. These low-level winds are associated with the surface high pressure systems in the atmosphere above the eastern subtropical ocean areas, as shown in Fig. 6.18. The wind systems and the associated currents and cool SSTs are best developed during the summer in

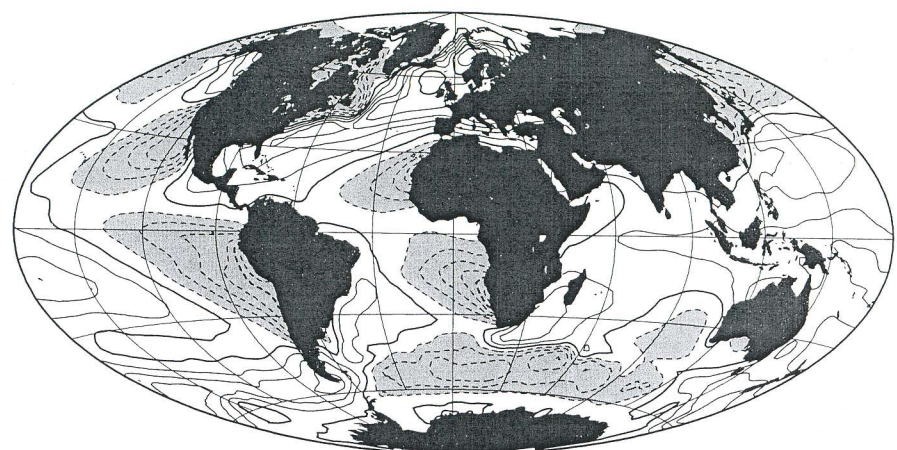


**Fig. 7.11** The deviation of the July sea surface temperature from its zonal average at each latitude. Contour interval is  $1^{\circ}\text{C}$ , and values less than  $-1^{\circ}\text{C}$  are shaded.

the Northern Hemisphere, and are more nearly year-round phenomena in the Southern Hemisphere. It is believed that the geometry of the coastlines in the two oceans, and in particular the northwest–southeast slope of the coastlines of South America and Africa, causes the eastern boundary currents in the Southern Hemisphere to be better developed and to extend to the equator and then westward along the equator. The cooler than average SST in eastern boundary current regions is often associated with atmospheric subsidence and persistent stratiform cloud [Fig. 3.21(b)].

#### 7.4.3 Interannual Variability in the Equatorial Pacific: ENSO

Large east-to-west gradients in SST and subsurface thermal structure exist in the tropical Pacific and Atlantic Oceans. These gradients are associated with the upwelling of cold water at the eastern margins of the oceans and along the equator in the eastern part of the basin. The thermocline is deepest in the western tropical oceans and rises toward the surface in the eastern equatorial regions where upwelling occurs (Fig. 7.12). The density and pressure gradients associated with the east–west slope of the thermocline in the Pacific are supported by the westward wind stress applied by the tropical easterly winds. Once every several years this balance is disrupted and warm water spreads toward the east, causing SST and climatic anomalies that may persist for a year or more. Such events are called *warm anomalies* of the tropical Pacific Ocean. If warm waters appear near the coast of South America, where the waters are normally very cold, the event is known locally as an *El Niño*. The appearance of warm waters at the coast of South America is associated with a deepening of the thermocline that normally intersects the surface of the eastern Pacific. Under normal

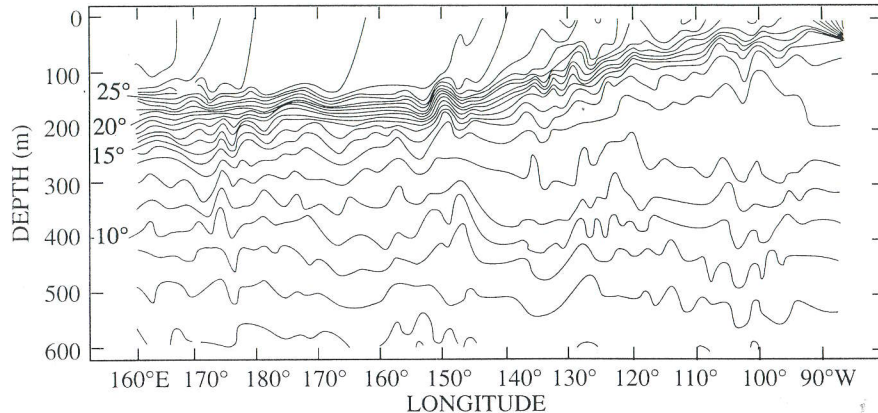


**Fig. 7.12** Thermal structure of the equatorial Pacific Ocean showing the slope of the thermocline ( $^{\circ}\text{C}$ ). [From Colin *et al.* (1971).]

conditions upwelling of cold, nutrient-rich water from below the thermocline supports a very rich fishery. Deepening of the thermocline during an El Niño cuts off the supply of nutrients to the surface, and the fishery off the coast of equatorial South America is adversely affected. Changes in the SST are coupled with changes in the convection and large-scale atmospheric flow in the tropics. The warming of the SST near the South American coast is often associated with substantial precipitation in what is otherwise a generally arid coastal climate. Changes in SST distribution in the central and western Pacific are associated with changes in the surface pressure and large-scale wind distributions, which can have effects that extend into middle latitudes. The related oceanic and atmospheric variations that accompany warm and cold events in the equatorial Pacific are referred to jointly as the *El Niño-Southern Oscillation* (ENSO) phenomenon.

## 7.5 Theories for Wind-Driven Circulations

### 7.5.1 The Ekman Layer, Wind-Driven Transport, and Upwelling

Because of the rotation of Earth, the frictional component of the vertically integrated transport of water in the surface layer of the ocean is not in the direction of the applied wind stress, but 90 degrees to the right of it in the Northern Hemisphere and 90 degrees to the left of it in the Southern Hemisphere. This wind-driven near-surface water transport plays a critical role in determining the relatively cold surface temperatures in the eastern boundary current regions and along the equator, and it also plays an important role in driving the subtropical gyres that feed the western boundary currents.

To show the relationship between wind stress driving, currents, and transport we may consider a homogenous ocean of constant density and pressure, and assume that

## 7.5 Theories for Wind-Driven Circulations

it is driven by a uniform wind stress with eastward component  $\tau_x$  and northward component  $\tau_y$ . We seek a steady solution in which frictional stresses and Coriolis accelerations are in balance.<sup>1</sup>

$$fv = -v \frac{d^2 u}{dz^2} \quad (7.1)$$

$$fu = v \frac{d^2 v}{dz^2} \quad (7.2)$$

The *Coriolis parameter* ( $f = 2\Omega \sin \phi$ ) measures twice the local vertical component of the rotation rate ( $\Omega$ ) of Earth. The frictional forces have been described such that the frictional stress is proportional to the shear of the current velocity times a momentum diffusion coefficient  $v$ . The specified wind stress thus enters as a boundary condition on the current shear at the surface, and we assume that the current goes to zero at large depths, so that the boundary conditions on (7.1) and (7.2) are

$$\left. \begin{aligned} v \frac{du}{dz} &= \frac{\tau_x}{\rho_o} \\ v \frac{dv}{dz} &= \frac{\tau_y}{\rho_o} \end{aligned} \right\} \quad \text{at } z = 0; \quad u = v = 0 \text{ at } z \rightarrow -\infty \quad (7.3)$$

where  $\rho_o$  is the density of the seawater and assumed constant. The solution for the velocities under these conditions is

$$u_E = \frac{e^{\delta z}}{\rho_o \sqrt{fv}} \left\{ \tau_y \cos\left(\delta z + \frac{\pi}{4}\right) + \tau_x \cos\left(\delta z - \frac{\pi}{4}\right) \right\} \quad (7.4)$$

$$v_E = \frac{e^{\delta z}}{\sqrt{fv}} \left\{ \tau_y \cos\left(\delta z - \frac{\pi}{4}\right) - \tau_x \cos\left(\delta z + \frac{\pi}{4}\right) \right\} \quad (7.5)$$

$$\text{where } \delta = \sqrt{f/2v} = z_E^{-1}.$$

The steady solution (7.4)–(7.5) describes the Ekman spiral. The current vector has its maximum magnitude at the surface where it is directed at an angle of  $\pi/4$  ( $45^{\circ}$ ) to the right of the wind stress vector in the Northern Hemisphere ( $f > 0$ ). The current vector turns toward the right with increasing depth, and its magnitude decreases exponentially with depth. The magnitude of the current decreases by a factor of  $e^{-1}$  for every increase of depth equal to  $z_E = \delta^{-1} = \sqrt{2v/f}$ .<sup>2</sup> If we integrate the currents over the depth range in which the currents are significant, we obtain the integrated transport in the Ekman layer.

$$U_E = \int_{-\infty}^0 u_E \, dz = \frac{\tau_y}{\rho_o f}; \quad V_E = \int_{-\infty}^0 v_E \, dz = -\frac{\tau_x}{\rho_o f} \quad (7.6)$$

<sup>1</sup>See, e.g., Gill (1982).

<sup>2</sup>An appropriate value of  $v = 30 \text{ m}^2 \text{ s}^{-1}$  gives an Ekman depth of  $\sim 800 \text{ m}$ .

The net horizontal water transport in the Ekman layer is directed at a 90° angle to the right of the applied wind stress in the Northern Hemisphere, so that if the wind stress is toward the east at the surface ( $\tau_x > 0$ ), the Ekman layer transport is toward the south ( $V_E < 0$ ). If a westward wind stress is applied near the equator, the Ekman layer transport will be northward in the Northern Hemisphere and southward in the Southern Hemisphere, because of the change of sign of  $f$  at the equator, so that a net divergence of surface flow will be generated. Conservation of mass requires upwelling along the equator to balance the Ekman layer transport away from the equator. The cold tongue of SST in the eastern equatorial Pacific Ocean during July [Fig. 7.10(b)] is caused largely by this wind-driven upwelling. The cold SST anomalies associated with the eastern boundary currents (Fig. 7.11) are associated with offshore Ekman transport driven by equatorward alongshore surface winds. Offshore Ekman transport near an ocean boundary requires upwelling to replace the exported water. Since water temperatures decrease with depth, upwelling is generally accompanied by cold sea-surface temperatures.

Wind stress driving can also cause vertical motions in the open ocean away from boundaries and the equator, if the wind stress has spatial gradients. If we consider the mass continuity equation for an incompressible fluid

$$\frac{\partial u}{\partial x} + \frac{\partial v}{\partial y} + \frac{\partial w}{\partial z} = 0 \quad (7.7)$$

and integrate it over the depth of the Ekman layer, we can derive a relationship between the applied wind stress and the vertical motion at the base of the Ekman layer.

$$w_E(-\infty) - w_E(0) = \int_{-\infty}^0 \left( \frac{\partial u_E}{\partial x} + \frac{\partial v_E}{\partial y} \right) dz \quad (7.8)$$

Utilizing (7.6) in (7.8) and assuming that the vertical current vanishes at the surface yields an expression for the vertical velocity at the bottom of the Ekman layer in terms of the wind stress applied at the surface. We obtain

$$w_E = \frac{\partial}{\partial x} \left( \frac{\tau_y}{\rho_o f} \right) - \frac{\partial}{\partial y} \left( \frac{\tau_x}{\rho_o f} \right) = \vec{k} \cdot \vec{\nabla} \times \left( \frac{\vec{\tau}}{\rho_o f} \right) \quad (7.9)$$

where  $\vec{\tau} = \vec{i} \tau_x + \vec{j} \tau_y$ , and  $\vec{i}$ ,  $\vec{j}$ , and  $\vec{k}$  are unit vectors in the eastward, northward, and upward directions respectively. The vertical velocity at the base of the Ekman layer in the open ocean is thus seen to be proportional to the curl of the wind stress vector divided by the Coriolis parameter. Where lateral boundaries are present, the dependence of upwelling on the wind stress is more complex, but wind stress near boundaries can produce large upwelling even without significant wind stress curl.

### 7.5.2 Sverdrup Flow and Western Boundary Currents

To understand the large-scale response of the ocean to wind stress forcing it is useful to consider the balance of vorticity in the ocean. *Vorticity* is the curl of the velocity

vector and is a measure of the local rotation of the fluid. For the large-scale motions of the atmosphere and the ocean it is the vertical component of absolute vorticity that is of most interest.<sup>3</sup>

$$\zeta_a = 2\Omega \sin \phi + \vec{k} \cdot \vec{\nabla} \times \vec{V} = f + \zeta_r \quad (7.10)$$

The absolute vorticity is the sum of planetary vorticity ( $f$ ), which is associated with the rotation of Earth, and relative vorticity ( $\zeta_r$ ), which is associated with the fluid motion relative to the surface of Earth. For flow without friction, the absolute vorticity remains constant unless a parcel of fluid changes its shape. If a parcel of fluid maintains its shape while moving equatorward to a latitude where Earth's rotation is less, then the fluid parcel must exhibit a change in relative vorticity in order to maintain a constant absolute vorticity. Stretching of fluid parcels along the direction of the rotation vector will cause the absolute rotation rate to increase.

The famous oceanographer H. U. Sverdrup showed that in the interior of the ocean an approximate balance exists between the meridional advection of planetary vorticity and the stretching of planetary vorticity by divergent motions:

$$\beta v = f \frac{\partial w}{\partial z} \quad (7.11)$$

where  $\beta = \partial f / \partial y$ . If we integrate (7.11) from the bottom of the ocean to the bottom of the Ekman layer and use (7.9), we obtain

$$\beta V_I = f \vec{k} \cdot \vec{\nabla} \times \left( \frac{\vec{\tau}}{\rho_o f} \right) \quad (7.12)$$

where

$$V_I = \int_{-D_o}^{-z_E} v dz \quad (7.13)$$

and it has been assumed that the Ekman layer is thin compared to the depth of the ocean, and that the vertical velocity is zero at the bottom of the ocean, where  $z = -D_o$ .

If we add the interior meridional transport velocity (7.13) to the Ekman layer meridional transport in (7.6) we obtain

$$V_I + V_E = \frac{1}{\beta} \vec{k} \cdot \vec{\nabla} \times \left( \frac{\vec{\tau}}{\rho_o} \right) \quad (7.14)$$

so that the total meridional mass transport is proportional to the curl of the wind stress.

If we consider the ocean circulation between the tropics and midlatitudes, the

<sup>3</sup>See, e.g., Pedlosky (1987).

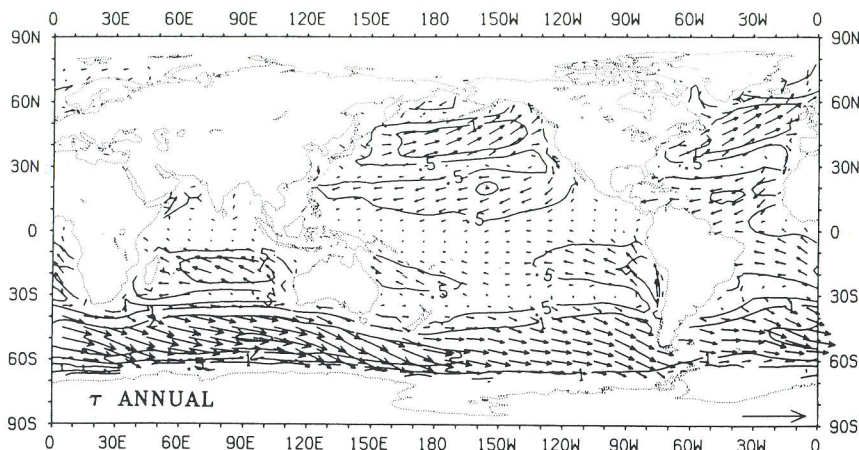


**Fig. 7.13** Annual mean wind stress over the global oceans depicted as vectors. The arrow at bottom right corresponds to  $5 \text{ dyn cm}^{-2}$  and contours of magnitude of 0.5, 1, 2, and  $3 \text{ dyn cm}^{-2}$  are plotted ( $1 \text{ dyn cm}^{-2} = 0.1 \text{ N m}^{-2}$ ). [From Trenberth *et al.* (1990). Reprinted with permission from the American Meteorological Society.]

wind stress varies from westward in the tropical easterlies to eastward in the mid-latitude westerlies (Fig. 7.13). Thus a negative wind stress curl is applied to the ocean, and according to (7.14), we should expect the water transport in the ocean to be equatorward. Physically, the wind stresses are causing the water to rotate about a vertical axis in a direction that is opposite to the rotation of Earth. To maintain a steady state in the face of this application of anticyclonic rotation, water must drift toward lower latitudes. The reduction in absolute vorticity is thus expressed as a decrease in the planetary vorticity of fluid parcels, and a steady state with constant relative vorticity can be maintained.

According to (7.14), the meridional transport in the ocean will be equatorward everywhere, so long as the wind stress curl is negative. How, then, can the conservation of mass and vorticity be jointly satisfied if the wind stress curl is everywhere negative? How does the water transported equatorward return to high latitudes and close the circulation of mass and vorticity? The western boundary currents observed in the midlatitude oceans are the solution to this dilemma.

A simple model can be constructed by adding a lateral diffusion term to the vorticity equation (7.11) that produces a steady gyre circulation with the northward-flowing return current intensified along the western margin of the ocean basin,<sup>4</sup> much like the observed northward flow is intensified in the western boundary currents. As the water flows poleward along this western margin, the planetary component of vorticity ( $f$ ) increases because of its dependence on latitude. If the absolute vorticity of the fluid parcels were to be conserved, then their relative vorticity would

<sup>4</sup>Stommel (1948); Munk (1950); Pedlosky (1987).

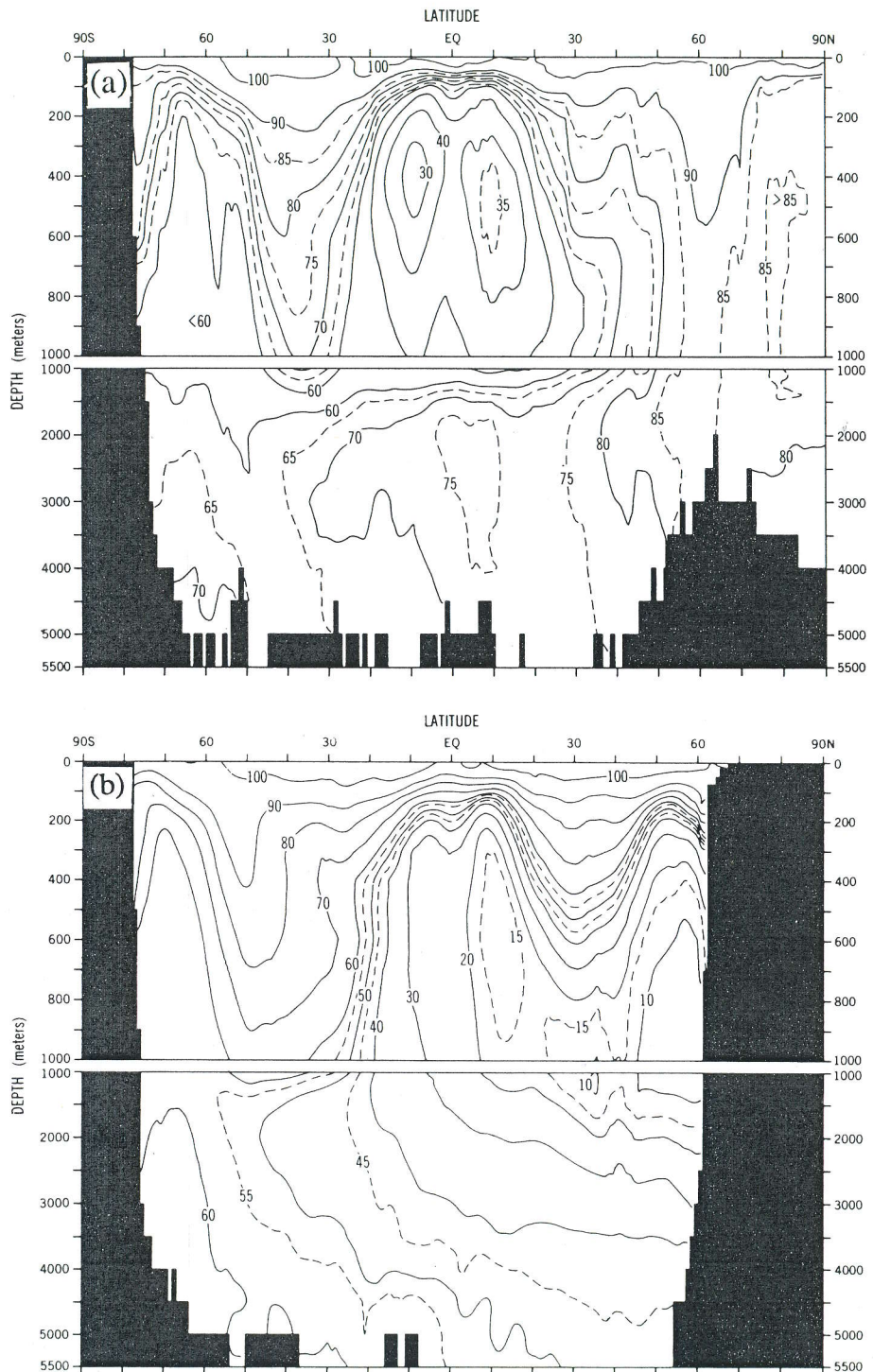
have to change to compensate for the increase in planetary vorticity. By flowing along the western margin of the ocean basin in a narrow current, the poleward return flow of the wind-driven circulation is able to collect enough vorticity in the same sense as Earth's rotation to arrive at middle latitudes with a vertical component of absolute vorticity near that of the planetary vorticity at these latitudes, so that the magnitude of the relative vorticity remains reasonably small and steady. In a simple linear model with lateral diffusion of momentum, the mechanism for collecting the necessary vorticity is through the lateral friction stresses, which generate vorticity of the proper sign only along the western boundary of the ocean basin. The warm, rapidly flowing western boundary currents of the Atlantic and Pacific Oceans are thus seen to be a response to the wind stress driving the bounded oceans of the Northern Hemisphere.

## 7.6 The Deep Thermohaline Circulation

The term *thermohaline circulation* is used to denote that part of the oceanic circulation that is driven by water density variations, which are in turn related to sources and sinks of heat and salt. It is traditional in oceanography to organize the discussion of the oceanic circulation into separate wind-driven and density-driven components, although the circulation of the ocean is not a simple addition of the effects of these two types of forcing. Wind driving influences the sources and sinks of heat and salt for the ocean by transporting surface water from the tropics to latitudes where cooling and evaporation can increase its density to very large values. The heat transport associated with the thermohaline circulation affects the SST gradients that help to drive atmospheric winds. Wind driving and density driving of the oceanic circulation are therefore very closely coupled and cannot be easily separated. It is generally true, however, that wind driving is the strongest influence on currents near the surface, and density driving dominates the flow at depth.

Below the thermocline there exist slow circulations driven primarily by density gradients in the deep ocean. These circulations are difficult to measure directly, since the currents associated with them are very weak, but their nature can be inferred from the distributions of trace constituents of seawater. Away from the surface, temperature and salinity of water masses change very slowly, so that the water masses and their origins can be inferred from the particular combination of temperature and salinity that characterizes them.

Most gases are soluble in water, so that the concentrations of particular gases can also be used to characterize water sources. The saturation concentration of a gas in seawater is the amount that would exist in solution at equilibrium, if seawater at a particular temperature and salinity were exposed to the gas. Saturation concentrations of gases in seawater increase as the water gets colder. For example, the saturation concentrations of oxygen and carbon dioxide in seawater at  $0^\circ\text{C}$  are about 1.6 and 2.2 times their values at  $24^\circ\text{C}$ , respectively. The concentration of oxygen in



surface water is always slightly greater than its saturation value, probably as a result of efficient mixing of bubbles of air into the surface water and production of oxygen in surface waters by photosynthesis. When surface water sinks into the deeper levels of the ocean its source of oxygen is cut off, and the oxygen is slowly consumed by bacteria as they feed on organic matter at depth. One may therefore use the depletion of the oxygen concentration below its saturation value as a measure of the time since the water has been at the surface.

Figure 7.14 shows the oxygen saturation versus depth and latitude in the Atlantic and Pacific Oceans. In the north Atlantic Ocean we observe that high saturation values extend to great depths, and that these high values extend toward the Southern Hemisphere at depths below  $\sim 1500$  m. We infer then that significant downwelling of water occurs in the north Atlantic and that this water sinks most of the way to the bottom of the ocean and then spreads southward. The distribution of oxygen saturation in the north Pacific Ocean is very different from that in the north Atlantic. In the north Pacific we see no evidence of downwelling, and in fact the oxygen at depth is severely depleted with saturations about 10–15% at latitudes and depths where the oxygen saturation is about 85% in the north Atlantic.

From the oxygen saturation alone we can infer that water from the surface sinks relatively quickly to the deep ocean in the north Atlantic, but that this does not occur in the Pacific. We cannot infer the full circulation of the deep ocean from oxygen alone, nor can we directly infer the subsidence rate, since the rate of oxygen depletion depends on the biological activity at depth, which in turn depends on the rate at which nutrients are supplied to them by deposition from above. The inferences from temperature, salinity, oxygen, and many other tracers suggest a deep-water circulation in the Atlantic like that shown in Fig. 7.15. A large mass of deep water is formed in the northern margin of the ocean, which then flows southward to fill a large fraction of the deep Atlantic (so-called north Atlantic deep water). This water rises toward the surface again in the vicinity of 60°S. Cold, but lower salinity water is formed in midlatitudes of the Southern Hemisphere and wedges itself between the warm surface water and the north Atlantic deep water below. Bottom water is formed around Antarctica, mostly in the Weddell Sea.

The mechanisms of deep-water formation in the north and south Atlantic are believed to be somewhat different. In the north Atlantic, warm, saline water flows poleward from midlatitudes, where the Gulf Stream provides an important source of such water. This water is carried farther poleward into the Norwegian and Greenland Seas, where it is exposed to very cold atmospheric temperatures. The cooling of this saline water produces water that is dense enough to sink to great depths. The surface water in high latitudes of the Southern Hemisphere is relatively fresh, because of the excess of precipitation over evaporation in those latitudes, and there is no warm

**Fig. 7.14** Oxygen saturation in percent for the (a) Atlantic and (b) Pacific Oceans. [From Levitus (1982).]

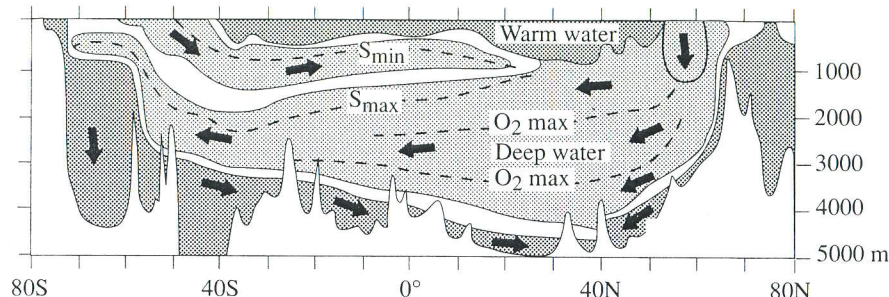


Fig. 7.15 Deep-water flow in the Atlantic Ocean inferred from temperature, salinity, and oxygen measurements. [Adapted from Dietrich *et al.* (1980). Reprinted with permission from Wiley and Sons, Inc.]

western boundary current to carry warm, saline water poleward, since the circum-polar current inhibits efficient transport of water from middle to polar latitudes in the southern oceans. Some saline water reaches the surface of the southern polar oceans by flowing southward at intermediate depths and rising at high latitudes in the south Atlantic. This water is also enhanced in nutrients, since it has spent some time at intermediate depths, where nutrients can be dissolved from falling detritus and photosynthetic organisms do not exist to consume the nutrients. In the Weddell Sea, which is the source region for much of the Antarctic bottom water, the formation of very dense water is more dependent on sea ice production. When ice is formed from seawater, salt is rejected from the crystal structure, resulting in the formation of brine, which adds salt to the water immediately under the ice and thereby increases its density. This cold, saline water is dense enough to sink to the bottom of the Atlantic.

To infer the rate of downwelling it is necessary to use tracers with known decay times such as carbon-14 ( $^{14}\text{C}$ ). Carbon-14 is a radioactive isotope produced naturally in the atmosphere by cosmic rays and by the explosion of atomic bombs in the atmosphere. Since the rate of decay of  $^{14}\text{C}$  to  $^{12}\text{C}$  is precisely known, the ratio of these isotopes can be used to estimate how long water has been below the surface. The rate and spatial distribution of downwelling can also be inferred from transient trace gases such as chlorofluorocarbons, which are man-made and have been introduced into the atmosphere only in the last 50 years or so.

By combining the evidence available from tracers of seawater movement it has been convincingly shown that at the present time deep ocean water is formed only at high latitudes in the north and south Atlantic. Only in these two locations can water of sufficient density be formed to sink to the deep ocean. From these two locations water spreads out at depth to fill the Pacific and Indian Oceans, where the water gradually rises toward the surface. Since the north Pacific is the farthest from either of these two locations, the water at intermediate depths in the north Pacific is the “oldest” ocean water in the sense that it has been the longest time since this water

was exposed to the atmosphere. The fact that the oldest water is not at the ocean bottom suggests that the deep water formed in the Atlantic slowly rises elsewhere, as would be required by the conservation of water mass. The regions of the ocean where deep water can be formed constitute a small fraction of the total surface area of the ocean. For example, 75% of the ocean has potential density greater than 27.4, but only 4% of the surface water has a density that high.<sup>5</sup> It is estimated that the time required to replace the water in the deep ocean through downwelling in the regions of deep water formation is on the order of 1000 years. We may call this the turnover time of the ocean. The thermal, chemical, and biological properties of the deep ocean therefore constitute a potential source of long-term memory for the climate system on time scales up to a millennium. Some chemical properties of the ocean take longer than one turnover time to change significantly, so that the potential exists for ocean memory on time scales longer than the ocean turnover time.

## 7.7 Transport of Energy in the Ocean

The general circulation of the ocean produces horizontal transport of energy from the tropics to the polar regions that is important for climate. It is not easy to measure this heat transport directly, however. It is difficult and expensive to obtain simultaneous current and temperature measurements from the surface to the bottom of the ocean. Such measurements require a ship or a large buoy and a cable with thermistors and current meters that extends from the surface to the ocean bottom, which is a distance of ~4 km on average. The spatial scales of the motions that are important for heat transport in the ocean are often small compared to the great expanse of an ocean basin, so that it is beyond our means to simultaneously measure current and temperature at enough spatial points and frequently enough in time to continuously monitor the product of velocity and temperature that produces most of the heat transport in the ocean. Attempts have been made to measure a series of profiles across a basin at a particular latitude, but these estimates must be assigned a rather large uncertainty.<sup>6</sup>

An alternative to direct measurement of currents and temperatures is to infer the heat transport of the ocean from the energy balance of Earth or of the ocean.<sup>7</sup> The change in the energy content of a region on Earth ( $\partial E_{\text{ao}}/\partial t$ ), following (2.19), is the excess of the net incoming radiation at the top of the atmosphere ( $R_{\text{TOA}}$ ) over the energy exported from that region by transport in the ocean and atmosphere ( $\nabla \cdot \vec{F}_{\text{ao}}$ ).

$$\frac{\partial E_{\text{ao}}}{\partial t} = R_{\text{TOA}} - \nabla \cdot \vec{F}_{\text{ao}} \quad (7.15)$$

<sup>5</sup>Sarmiento and Toggweiler (1984).

<sup>6</sup>Bryden and Hall (1980).

<sup>7</sup>Vonder Haar and Oort (1973); Oort and Vonder Haar (1976).

We may assume that the divergence of the horizontal transport can be decomposed into contributions from the atmosphere ( $\nabla \cdot \vec{F}_a$ ) and the ocean ( $\nabla \cdot \vec{F}_o$ ), and then rearrange (7.15) to obtain an expression for the divergence of transport in the ocean.

$$\nabla \cdot \vec{F}_o = R_{\text{TOA}} - \frac{\partial E_{\text{ao}}}{\partial t} - \nabla \cdot \vec{F}_a \quad (7.16)$$

To estimate the effect of ocean heat transport on the energy balance, we need to know the net radiation entering at the top of the atmosphere, the rate of local energy storage, and the rate at which the atmosphere is transporting energy out of the region. The net radiative energy input at the top of the atmosphere may be estimated from measurements taken from satellites. Mapped analyses of winds, temperatures, geopotential energy, and humidity from balloon and satellite measurements are good enough to give reasonable estimates of energy transport in the atmosphere. Storage of energy in the climate system can be estimated from observations, but if we average over an integral number of annual cycles, the energy storage is generally small and can be safely ignored. In this case we may use (7.15) and (7.16) to write

$$R_{\text{TOA}} = \nabla \cdot \vec{F}_{\text{ao}} = \nabla \cdot \vec{F}_a + \nabla \cdot \vec{F}_o \quad (7.17)$$

By integrating the net radiation over latitude, as described in Section 2.9, we may derive the required total meridional transport and subtract from it the atmospheric transport to obtain the oceanic transport.

$$\vec{F}_o = \vec{F}_{\text{ao}} - \vec{F}_a \quad (7.18)$$

Estimates of the total annual mean meridional energy transport required to balance the radiative forcing, atmospheric transport, and the oceanic transport are shown in Fig. 7.16. Such estimates imply that the maximum meridional energy transport by the oceans in the Northern Hemisphere is about the same magnitude as the atmospheric energy transport, but that it occurs at a lower latitude. The total required energy transport is nearly 6 petawatts (PW) and peaks near 45°N. The atmospheric transport has a broad maximum in middle latitudes at ~4 PW and the oceanic flux peaks near 20°N at ~3.2 PW. The total required energy transport is reasonably well measured, but the atmospheric and oceanic fluxes have uncertainties as large as 30% or ~1 PW. These large uncertainties notwithstanding, it is still interesting that the estimated ocean transport is not as sharply peaked in the Southern Hemisphere, and reaches a maximum there of only ~2 PW (1 PW =  $10^{15}$  W). It is possible that the ocean transports are different because of the different land-sea geometry in the two hemispheres and the more developed western boundary currents in the Northern Hemisphere.

The oceanic energy flux can also be estimated from the energy balance at the surface of the ocean. Following (4.1) the energy balance at the surface can be written

$$\nabla \cdot \vec{F}_o = R_s - LE - SH - \frac{\partial E_s}{\partial t} \quad (7.19)$$

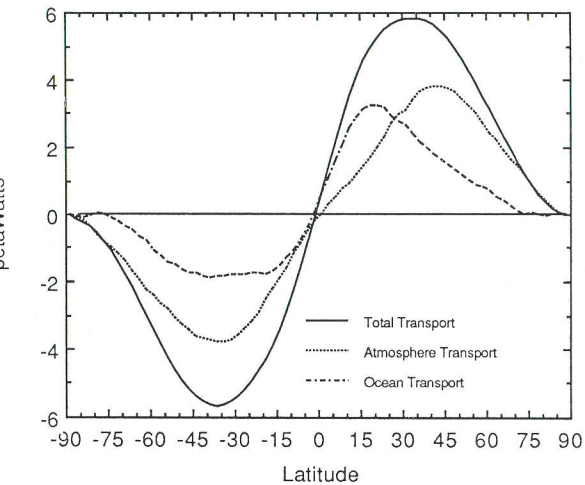


**Fig. 7.16** Estimates of the annual mean meridional energy transport required by the energy balance at the top of the atmosphere, estimated from observations in the atmosphere, and the oceanic transport obtained by subtracting the atmospheric energy transport from the total transport required by the annual energy balance (7.16). Net transport inferred from Earth Radiation Budget Experiment data. [Atmospheric transport data from Peixoto and Oort (1984). Used with permission from the American Physical Society.]

The divergence of energy transport in the ocean can be estimated from the ocean surface energy balance if the net radiative heating, the evaporative cooling, the sensible cooling, and the energy storage in the ocean can be estimated. All of these terms are discussed in Chapter 4, and maps of the inferred oceanic flux divergence appear in Fig. 4.18(d). Estimates of meridional energy transport in the ocean obtained from (7.19) are in general agreement with estimates derived from (7.16), in that they show a maximum transport by the oceans at about 20°N (Fig. 7.17). The magnitudes of the estimated transports are considerably less than those of the estimates derived from the residual in the planetary energy balance, however. The surface energy balance method can also provide estimates for individual regions and oceans. The estimates indicate that the Atlantic Ocean transports energy northward across the equator, while the Indian Ocean transports energy southward.

## 7.8 Mechanisms of Transport in the Ocean

The meridional transport of energy in the oceans is clearly important for climate, but because the transports are not measured directly it is uncertain what types of circulations contribute most to the transport. There are three generic types of circulations that are candidates: wind-driven currents, thermohaline circulations, and midocean eddies.

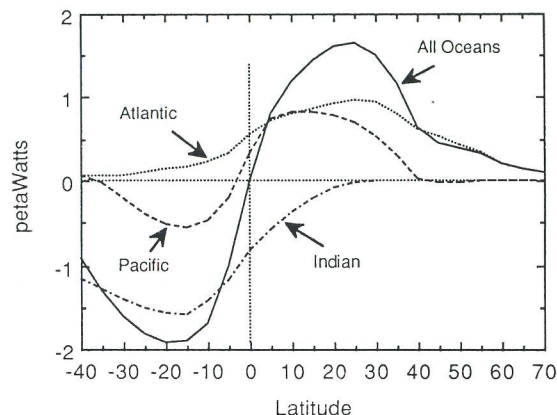


**Fig. 7.17** Estimates of the annual mean northward energy transport in the global ocean, and the Atlantic, Pacific, and Indian Oceans derived from the surface energy balance of the oceans (7.18). [Adapted from Hsiung (1985). Reprinted with permission from the American Meteorological Society.]

### 7.8.1 Wind-Driven Currents

The warm western boundary currents such as the Gulf Stream and the Kuroshio and their associated mid-ocean drift currents seem to play an important role in meridional energy transport in the oceans. The swift, warm currents that flow poleward along the western boundaries of the Atlantic and Pacific Oceans are capable of carrying large amounts of heat poleward. The equatorward flow of relatively cold water in eastern boundary currents also contributes to the poleward energy flux. We can estimate the poleward heat flux associated with the Gulf Stream by considering the product of the mass flux of water and the temperature difference between the Gulf Stream and the average near-surface temperature at the same latitude. The mass flow is the velocity of the current times its area and the water density. From Fig. 7.8(b) we estimate that the Gulf Stream is 60 km wide and 500 m deep and has an average current of  $1 \text{ m s}^{-1}$ . Assuming a density of  $10^3 \text{ kg m}^{-3}$ , we can obtain an estimate of the mass flux in the Gulf Stream of  $3.0 \times 10^{10} \text{ kg s}^{-1}$ .

$$\begin{aligned} \text{Density} \cdot \text{width} \cdot \text{depth} \cdot \text{speed} &= 10^3 \text{ kg m}^{-3} \cdot 60 \text{ km} \cdot 500 \text{ m} \cdot 1 \text{ m s}^{-1} \\ &= 3 \times 10^{10} \text{ kg s}^{-1} \end{aligned}$$

This estimate of 30 Sverdrups<sup>8</sup> agrees with more detailed calculations of the flow through the Florida Straits.<sup>9</sup> If we assume that the Kuroshio has a similar mass flux, then the total poleward mass flux in Northern Hemisphere western boundary currents is  $6 \times 10^{10} \text{ kg s}^{-1}$ . To calculate the energy flux associated with this mass transport,

<sup>8</sup>The Sverdrup ( $= 10^6 \text{ m}^3 \text{ s}^{-1}$ ) is the traditional oceanographic unit of water flow.

<sup>9</sup>Bryden and Hall (1980).

we need the heat capacity of water ( $4281 \text{ J K}^{-1} \text{ kg}^{-1}$ ) and the temperature difference between the poleward-flowing boundary currents and the equatorward-flowing water at the same latitude. We do not know this temperature difference precisely, and it is very dependent on whether the equatorward flow is above or below the thermocline. It is interesting to consider how big this temperature difference must be in order for the western boundary currents to produce a meridional heat transport of comparable magnitude to the maximum oceanic flux displayed in Fig. 7.16. To obtain an oceanic flux of 3.2 PW requires a temperature difference between the poleward-flowing and equatorward-flowing water of about  $12^\circ\text{C}$ .

$$\begin{aligned} c_w \rho_w v_w \text{area}_w \Delta T &= 4218 \text{ J K}^{-1} \text{ kg}^{-1} \cdot 6 \times 10^{10} \text{ kg s}^{-1} \cdot 12.6 \text{ K} \\ &= 3.2 \text{ petaWatts} \end{aligned}$$

From Fig. 7.8(a) we estimate the average temperature of the Gulf Stream water to be about  $22^\circ\text{C}$ . This is considerably warmer than the average temperature of the ocean at these latitudes, which is somewhere near  $5^\circ\text{C}$ . If the equatorward return flow is primarily in the interior below the thermocline, then it would be very easy to produce the observed oceanic heat flux with the western boundary currents and an associated colder interior return flow. In any case, it is reasonable to suppose that wind-driven western boundary currents play an important role in meridional energy transport in the oceans.

### 7.8.2 The Deep Thermohaline Circulation

The mass flow of the deep thermohaline circulation is governed by the rate at which deep water can be formed at high latitudes. In the Northern Hemisphere deep water is formed only in the Atlantic at high latitudes, and the formation rate is quite slow, since it takes several centuries to replace the deep water in the Atlantic. It is estimated that the average rate of deep-water formation in the North Atlantic is  $1.5 - 2 \times 10^{10} \text{ kg s}^{-1}$  and in the Antarctic Ocean about  $1 \times 10^{10} \text{ kg s}^{-1}$ . The deep thermohaline circulation is critical for the climate of the far North Atlantic and for deep heat storage, and it may be an important contributor to the energy flow across  $20^\circ\text{N}$ .

### 7.8.3 Mid-ocean Eddies

The Gulf Stream and the Kuroshio spin off long-lived eddies via baroclinic and barotropic instabilities (Fig. 7.9). These are the oceanic analogs to the eddies that produce most of the atmospheric meridional energy transport in midlatitudes. The role of eddies for heat transport in the ocean is likely much less than in the atmosphere, however, because of their smaller spatial scales compared with the scale of the oceans. Moreover, the oceanic eddies are best developed well poleward of the latitude of the maximum oceanic transport. The wind-driven and thermohaline circulations are likely to provide much more important contributions to the meridional heat flux in the subtropics.

**Exercises**

1. Use the data in Figs. 7.1 and 7.2 to estimate how much the salinity of the surface water of the Arctic Ocean would need to increase before the surface density would equal the potential density at 1000-m depth. How does this compare with the average salinity of the ocean?
2. What depth of seawater would need to freeze in the Arctic Ocean to produce the increase in salinity of problem 1 in the top 100 m of water? Assume that all salt is rejected from sea ice and enters the 100-m layer.
3. With the negative wind stress curl characteristic of today's climate, the wind-driven meridional flow (7.14) is an equatorward drift, which we can hypothesize occurs mostly in the thermocline or above it. How would the net heat transport produced by this drift and its return flow be different if, rather than a warm western boundary jet, the return flow were a slow poleward drift near the bottom of the ocean?
4. Discuss the ways in which the extension of the warm, saline Gulf Stream into the Norwegian and Labrador Seas assists in the formation of dense water that can sink to the depths of the Atlantic Ocean.
5. Use Fig. 7.2 to estimate the initial and final density values of a kilogram of water that starts in the tropics with a temperature of 28°C and a salinity of 35‰ and flows on the surface in the Gulf Stream to the Norwegian Sea, where it arrives with a temperature of -1°C. Assume the water conserves its salinity en route and loses heat by sensible heat transfer.
6. As an alternative to problem 5, assume that the kilogram of water starts in the tropics, but is cooled by evaporation along its route rather than by sensible heat loss. Estimate the mass of water that is lost by evaporation en route, if the parcel arrives in the Norwegian Sea with a temperature of -1°C. Calculate the salinity on arrival, assuming that no horizontal mixing or precipitation occurs, and the salinity is well mixed through the top 100 m of the ocean. What is the density on arrival? When you compare the final density with that obtained in problem 5, is the effect of evaporation on the final density significant? Is it important to know the Bowen ratio for the parcel along its route?
7. Suppose that a wind stress is applied to the ocean, taking the following simple form.

$$\tau_x = \begin{cases} A \cos\left(\frac{\pi y}{L}\right) & -L < y < L \\ A & |y| > L \end{cases}$$

Derive an equation for the vertical velocity at the bottom of the Ekman layer assuming a constant Coriolis parameter  $f = f_o = 2\Omega \sin 30^\circ$ . Derive an equation for the integrated meridional transport  $V_I$ , using (7.12) with the  $f$  and  $\beta$  appro-

priate for 30°N latitude. Determine a numeric value for the maximum  $w_E$  and  $V_I$  using the following constants:  $A = 2 \text{ dyn cm}^{-2} = 0.2 \text{ N m}^{-2}$ ,  $L = 1500 \text{ km}$ ,  $\rho_o = 1025 \text{ kg m}^{-3}$ . Plot  $\tau_x$ ,  $w_E$ , and  $V_I$  on the interval  $-L < y < L$ . Assuming that the ocean basin is 5000 km wide, calculate the water mass flux at 30°N associated with the interior flow. Compare this number with the estimate for the Gulf Stream mass flux given in Section 7.8.